Available online at www.sciencedirect.com
SCIENCE DIRECT
Journal of the European Ceramic Society 26 (2006) 2503–2510
www.elsevier.com/locate/jeurceramsoc

Low temperature synthesis of anorthite based glass-ceramics via sintering and crystallization of glass-powder compacts

V.M.F. Marques [a], D.U. Tulyaganov [a,b], S. Agathopoulos [a], V.Kh. Gataullin [b], G.P. Kothiyal [c], J.M.F. Ferreira [a,*]

[a] *Department of Ceramics and Glass Engineering, University of Aveiro, CICECO, 3810-193 Aveiro, Portugal*
[b] *Scientific Research Institute of Space Engineering, 700128 Tashkent, Uzbekistan*
[c] *Technical Physics and Prototype Engineering Division, Bhabha Atomic Research Centre, Mumbai 400085, India*

Received 3 April 2005; received in revised form 8 June 2005; accepted 24 July 2005
Available online 16 September 2005

Abstract

Anorthite based glass-ceramics were synthesized. The investigated glass compositions are located close to the anorthite-rich corner of the fluorapatite–anorthite–diopside ternary system. Glass powder compacts with mean particle size of 2 and 10 μm were prepared. Sintering behaviour, crystallization and the properties of glass-ceramics were investigated between 800 and 950 °C. In the case of specimens made from the finer particles, complete densification was achieved at a remarkably low temperature (825 °C) and the highest mechanical strength was obtained at 850 °C, but density significantly decreased at higher temperatures. The samples prepared from the larger particles exhibited higher values of density, shrinkage and bending strength within a wider temperature range (825–900 °C). Anorthite was predominantly crystallized between 850 and 950 °C, along with traces of fluorapatite. Diopside was detected only in the MgO richer compositions.

Keywords: Sintering; Crystallization; Microstructure-final; Glass-ceramics; Anorthite

1. Introduction

Low temperature co-fired ceramic (LTCC) packages have been extensively investigated to achieve high signal propagation speed, reliability and low cost.[1–3] Anorthite is a potential material for LTCC substrates due to its lower coefficient of thermal expansion and lower dielectric constant than alumina.[4] In these applications, sintering of ceramics should occur at about 950 °C, which is lower than the melting points of cupper, silver or gold, since the use of metals results in less heat generation during operation due to their high thermal conductivity.[5]

To fabricate anorthite glass-ceramics suitable for LTCC substrates and with high mechanical properties, complete densification should precede a sufficiently good crystallization.[6] Nevertheless, there is poor literature documentation on the mechanical properties of anorthite glass-ceramics.

Several studies have addressed their interest on sintering and crystallization of glass-powder compacts which correspond to stoichiometric anorthite.[6–10] Thus, it has been found that B_2O_3 enhances sinterability, while TiO_2 increases the dielectric constant of anorthite ceramics.

Leonelli et al.[11] have investigated the nucleation and the crystallization mechanisms of three glass compositions which belong to the anorthite–diopside system. The theoretical wt.% ratio of anorthite/diopside (An/D) was 75/25, 50/50 and 25/75. Complete densification was attained with no addition of nucleating agents. In the ceramized state of the composition with 75/25 ratio, anorthite was predominantly and easily formed even upon quenching from the melt, impeding the formation of pure glassy samples. Therefore, the tendency for crystallization actually makes difficult the control of sintering and crystallization processes.

* Corresponding author. Tel.: +351 234 370242; fax: +351 234 425300.
E-mail address: jmf@cv.ua.pt (J.M.F. Ferreira).

0955-2219/$ – see front matter © 2005 Elsevier Ltd. All rights reserved.
doi:10.1016/j.jeurceramsoc.2005.07.055

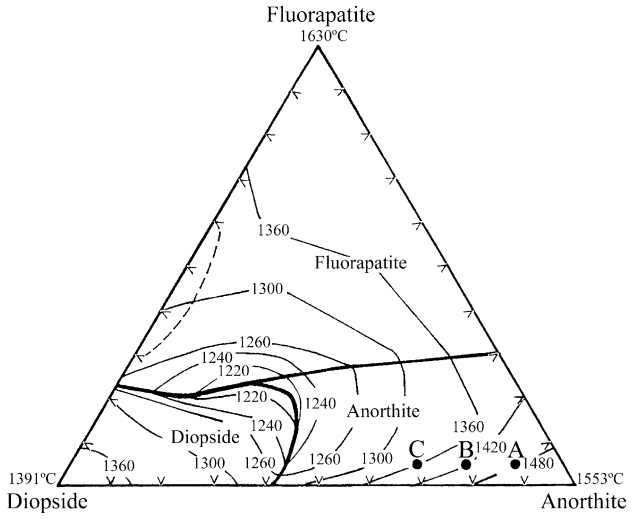

Fig. 1. The investigated compositions A, B and C in the fragment of fluorapatite–diopsite–anorthite ternary diagram (in wt.%)[12] (without considering the doping with B_2O_3).

Table 1
Chemical batch compositions A, B and C (wt.%)

Composition	SiO_2	Al_2O_3	CaO	MgO	P_2O_5	CaF_2	B_2O_3
A (An90-D10)	40.28	29.91	21.09	1.69	1.92	0.35	4.76
B (An80-D20)	41.78	26.85	21.82	3.40	1.94	0.36	3.85
C (An70-D30)	43.34	23.70	22.56	5.17	1.96	0.36	2.91

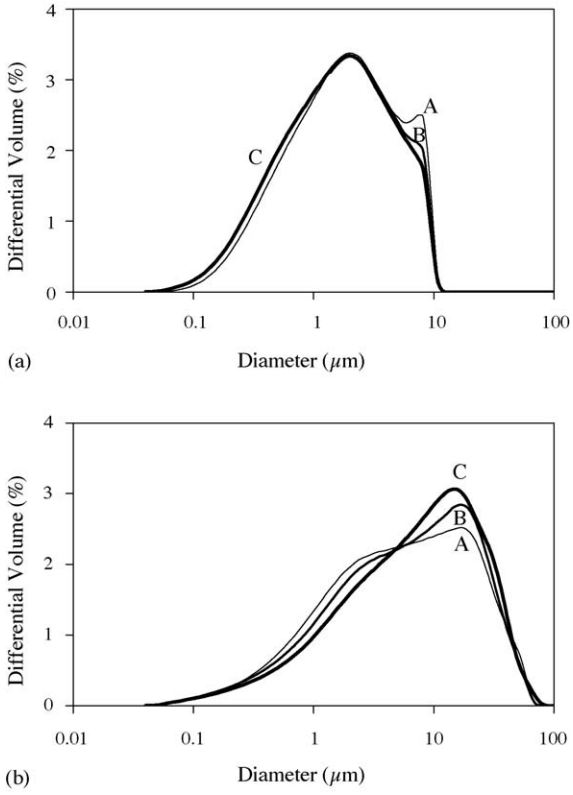

Fig. 2. Particle size distributions of the initial glass powders with mean particle sizes of ~2 μm (a) and ~10 μm (b).

Earlier thorough studies[12,13] on the phase equilibria in the fluorapatite–anorthite–diopside ($Ca_5(PO_4)_3F$–$CaAl_2Si_2O_8$–$CaMgSi_2O_6$) ternary system demonstrated that fluoarapatite beneficially aids the widening of glass-forming region at the anorthite–diopside boundary. On the base of these studies, this work presents the synthesis and characterization of anorthite based glass-ceramics using glass compositions located close to the anorthite-rich corner of the ternary system of Fig. 1 (points A, B and C). To enhance both melts' fluidity and sinterability of glass-powder compacts, the compositions were doped with B_2O_3. Form the liquidus lines plotted in Fig. 1, the liquidus temperatures of the compositions A, B and C (without considering the addition of B_2O_3) would be 1480, 1420 and 1360 °C, respectively. These compositions correspond to the anorthite/diopside weight ratios given in parentheses: A (An90-D10), B (An80-D20) and C (An70-D30), which will be hereafter used as the compositions' codes (Table 1). To evaluate the potential of the synthesized materials for LTCC applications, the influence of the particle size of the powders (~2 and ~10 μm) and of the temperature of heat treatment on several properties was investigated.

2. Materials and experimental procedure

Powders of technical grade of silicon oxide (purity >99.5%) and of calcium carbonate (>99.5%), and reactive grade Al_2O_3, CaF_2 and $NH_4H_2PO_4$ were used. According to the batch compositions shown in Table 1, homogeneous mixtures of batches (~100 g), obtained by ball milling, were preheated at 1000 °C for 1 h for decarbonization. Melting in Pt crucibles was carried out in air at 1580 °C for composition A, at 1550 °C for composition B and at 1500 °C for composition C (1.5 h dwelling time at maximum temperatures).

Glass frits were obtained by quenching of melts into cold water. The frits were dried and then milled in a high-speed porcelain mill in absolute ethanol media. Glass powders with the mean particle size of ~2 μm (Fig. 2a) and ~10 μm (Fig. 2b) were obtained after 3.5 h and 30 min milling, respectively. Rectangular bars (4 mm × 5 mm × 50 mm) were prepared by uniaxial pressing (80 MPa). The bars were subjected in heat treatment at 800, 825, 850, 900 and 950 °C (heating rate of 5 K/min; soaking for 1 h at the sintering temperatures).

The following techniques were used. The particle size distribution of the powders was determined by light scattering technique (Coulter LS 230, UK, Fraunhofer optical model). Differential thermal analysis (DTA) was carried out in air (Labsys Setaram TG-DTA/DSC, France; heating rate 5 K/min). The thermal expansion of sintered and crystallized samples was measured by dilatometric analysis (Bahr Thermo Analyse DIL 801 L, Germany; heating rate of 5 K/min; cross section of samples 4 mm × 5 mm). The crystallized phases were identified by X-ray diffraction (XRD, Rigaku Geigerflex D/Mac, C Series, Cu K_a radiation,

Japan). Microstructure observations and elemental analysis (SEM/EDS, Hitachi S-4100, Japan, 25 kV acceleration voltage) were carried out at polished and then chemically etched glass-ceramic surfaces by immersion in 2 vol.% HF solution for 4 min for the composition A and 8 min for the compositions B and C. The apparent density was measured by the Archimedes method (i.e. immersion in ethylenoglycol). Flexural strength (three-point bending) was measured with parallelepiped bars (Shimadzu Autograph AG 25 TA, 0.5 mm/min displacement; the presenting results are the average of 12 bars with a volume of 3 mm × 4 mm × 40 mm). Water absorption was measured according to the ISO-standard 10545-3, 1995. The linear shrinkage during sintering was also calculated from the dimensions of the green and of the sintered samples.

3. Results and discussion

All the investigated compositions were successfully melted and easily cast. The quenched glass frits were bubble-free, transparent and colourless with no visible crystalline inclusions, as was also confirmed by X-ray analyses which exhibited broad amorphous bands in the spectra.

The results of DTA, plotted in Fig. 3 and summarized in Table 2, indicate that the investigated glasses followed the typical events of vitreous materials that transform into glass-ceramics. A slight decrease of transition temperature (T_g), denoted by the endothermic depressions before crystallisation peaks, was observed from compositions A, B and C. A single exothermic crystallisation peak (T_{C1}) was registered in compositions A and B. This peak is seemingly split ($T_{C1}$and T_{C2}) in composition *C*. The increase of the mean particle size caused a shift of the crystallization peak maxima to higher temperatures and the height of the peaks was reduced. The aforementioned dependence of the thermographs on the particle size indicates that surface crystallization is the dominant mechanism in the investigated compositions.[10,11,14,15]

The shift of T_g to higher temperatures due to increasing amount of anorthite can be possibly interpreted in the light of the work of Barbieri et al.,[16] who attributed the shift of T_g and T_C to higher temperatures over increasing alumina-content to the role of Al^{3+} as a network former. The Al^{3+} cations form tetrahedral sites in the glass structure, which then cause polymerization of glass network and increase the viscosity of the glass.

The influence of the temperature of heat treatment on density, water absorption and shrinkage is plotted in Figs. 4 and 5. Sintering of glass-ceramics generally starts at temperatures slightly higher than T_g and takes place due to viscous flow, which instigates coalescence of powder and removes the pores from the bulk of materials.[6,17] The use of special additives, such as B_2O_3, and fine glass powders can enhance

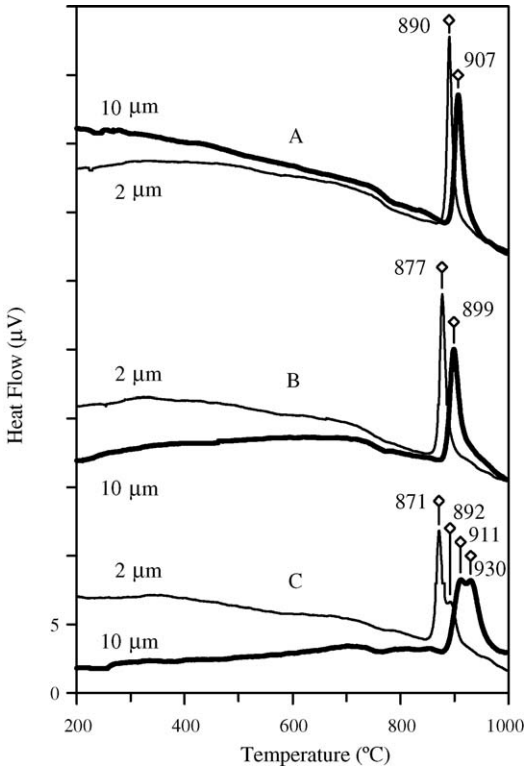

Fig. 3. Differential thermal analysis (DTA) of the investigated glasses.

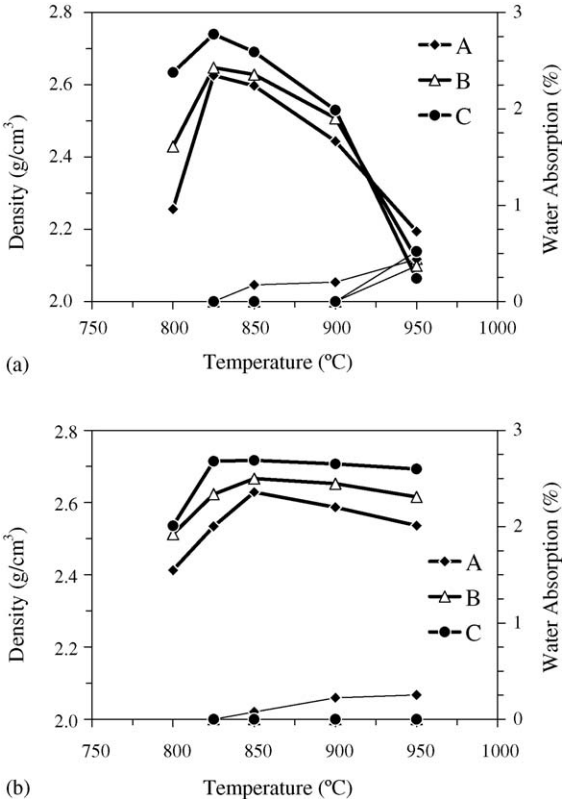

Fig. 4. Influence of the temperature of heat treatment on density (thick lines) and water absorption (thin lines) of samples made of powders with mean particle sizes of (a) 2 µm and (b) 10 µm. The standard deviation of the presenting points was less than 5%.

Table 2
Characteristic temperatures obtained from DTA (Fig. 3)

	A (An90-D10)		B (An80-D20)		C (An70-D30)	
	2 μm	10 μm	2 μm	10 μm	2 μm	10 μm
T_g (°C)	755	770	745	761	738	753
T_{C1} (°C)	890	907	877	899	871	911
T_{C2} (°C)	Not registered		Not registered		892	930

sinterability.[10,18] The highest values of density and shrinkage along with zero water absorption were obtained at 825 and 850 °C for the samples made from powders with mean particle sizes of 2 and 10 μm, respectively.

Sintering was completed at 850 °C for the samples made of finer powders (2 μm). Density significantly decreases at higher temperatures (Fig. 4a). The samples made of the coarser particles (10 μm) exhibited quite stable values of density and shrinkage within a wide temperature range from 825 to 900 °C (Figs. 4b and 5b). According to the DTA-plots (Fig. 3), the crystallization of the powders with size of 2 μm always peaked at lower temperatures than the 10 μm ones (i.e. crystallization occurs earlier in 2 μm than in 10 μm). Meanwhile, there is often a difference between the densities of the crystalline and the glassy phases. We have tackled this phenomenon in an earlier study on akermanite-diopside glass-ceramics,[19] where the crystallization of the glass can result in denser ceramic phases and thus secondary porosity can be developed in the bulk of the samples. In the present study, together with the reduced density, the plots of water absorption may further confirm this type of secondary porosity developed at 850–900 °C, more pronouncedly in the samples made of 2 μm sized powders (Fig. 4). Further increase of temperature beyond 900 °C probably causes dissolution phenomena where the larger particles (10 μm) are expected to exhibit higher resistance to melt than the smaller ones (2 μm). Therefore, the density of the samples made of powders of 2 μm dramatically decreases (Fig. 4a).

Fig. 6 shows that bending strength increases with increasing sintering temperature from 800 to 850 °C. Up to 900 °C, there is no significant difference between the samples made of finer and coarser glass powders. With regard to composition, mechanical strength generally increases in the order A < B < C. The maximum values for the compositions A, B

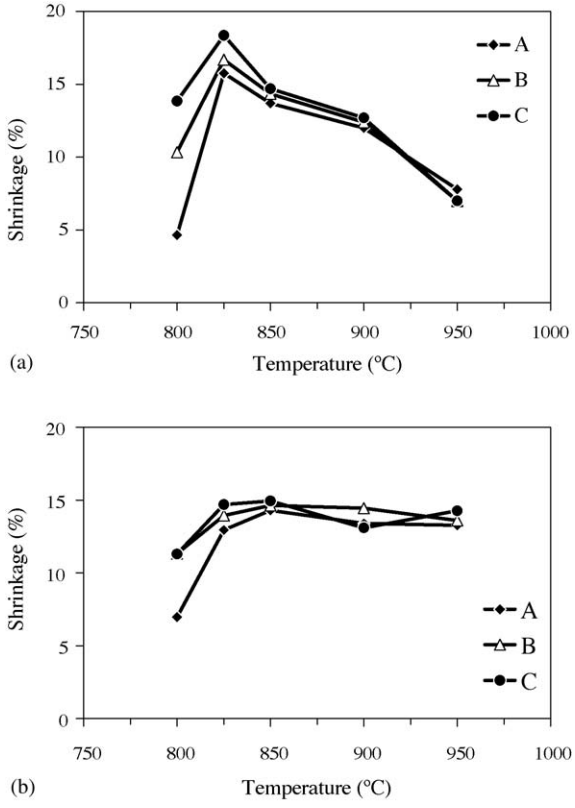

Fig. 5. Influence of the temperature of heat treatment on shrinkage of samples made of powders with mean particle sizes of (a) 2 μm and (b) 10 μm. The standard deviation of the presenting points was less than 5%.

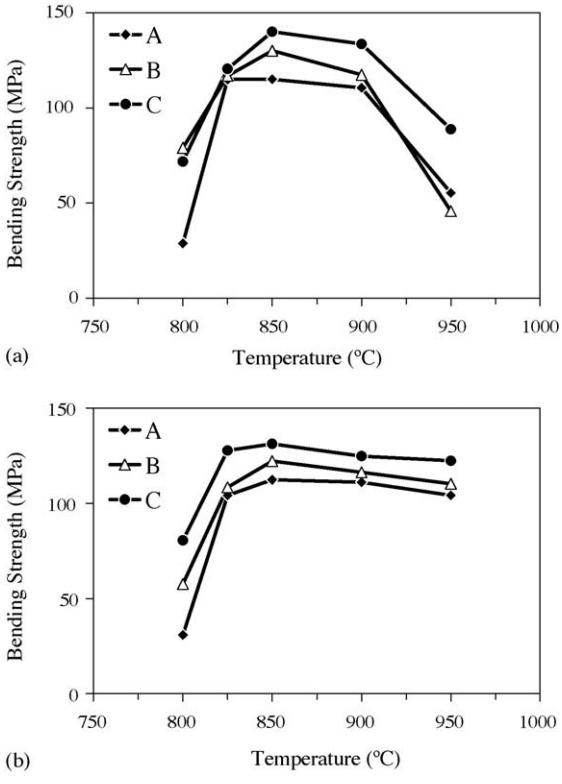

Fig. 6. Influence of the temperature of heat treatment on 3-point bending strength of samples made of powders with mean particle sizes of (a) 2 μm and (b) 10 μm. The standard deviation of the presenting points was less than 5%.

and C were 112–115 MPa, 122–130 MPa and 131–140 MPa, respectively.

According to the X-ray spectra (Fig. 7), triclinic anorthite was predominantly crystallized at 850–950 °C in all compositions investigated. The particle size did not affect the position of the X-ray peaks but a slight increase of peaks' intensity was observed with increasing particle size (thus only the spectra of the samples made of powders of mean particles size of 10 μm are shown in Fig. 7). Small peaks assigned to fluorapatite were registered in the spectra of composition A at all investigated temperatures (Fig. 7a). In composition B, diopside was further detected, and the relevant X-ray peaks were

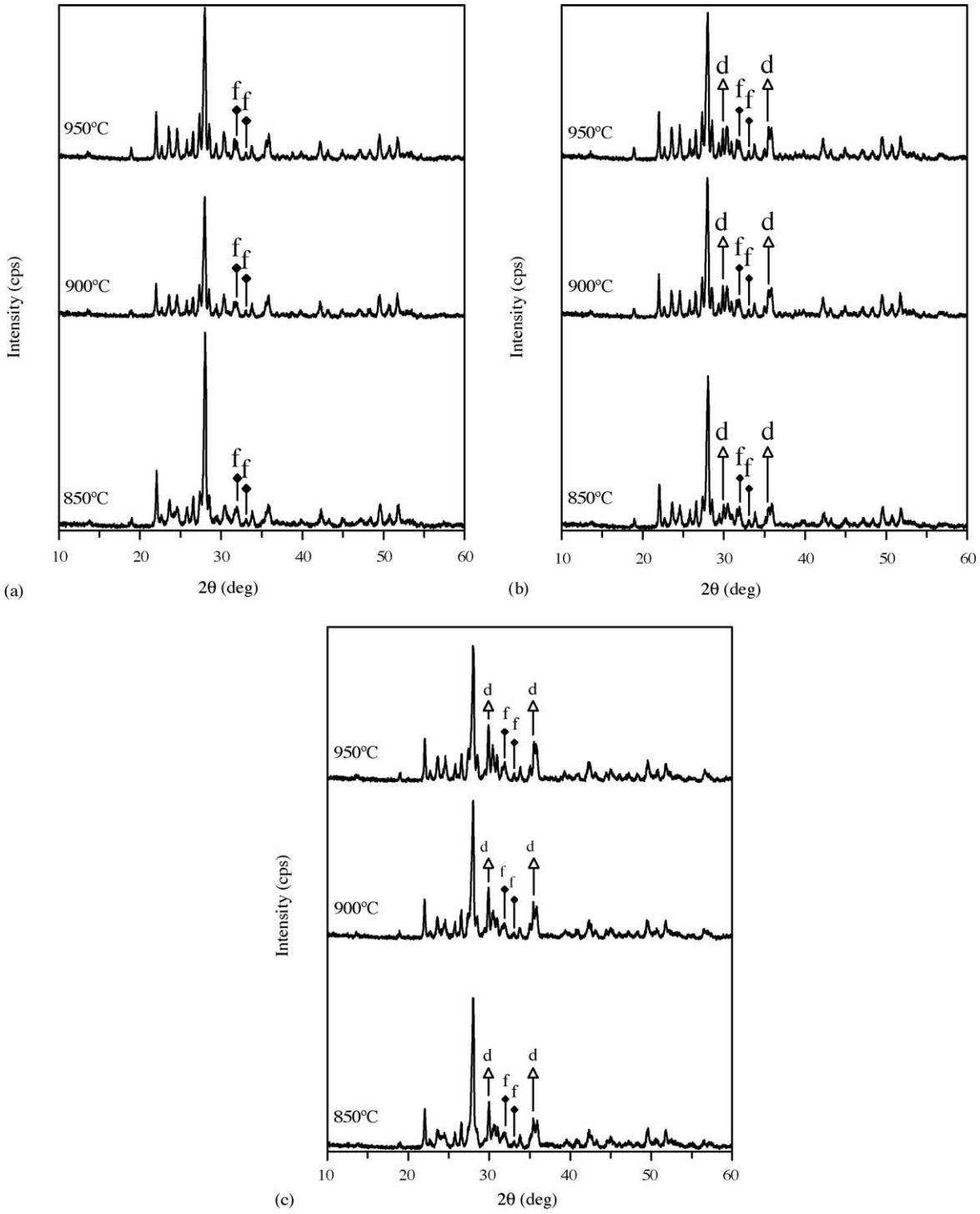

Fig. 7. XRD spectra of glass-ceramics (a) A, (b) B and (c) C. All the peaks fit to anorthite (41-1486) except those assigned to fluorapatite (f: 73-1727) and diopside (d: 75-1577). The spectra have not been normalized; full scale 10,000 cps.

intensified over increasing temperature (Fig. 7b). The presence of diopside was sounder in composition C, which is the richest in MgO (Fig. 7c), being in a fair agreement with the clear splitting of the exothermic peak (T_{C1} and T_{C2}) in the corresponding DTA thermograph of Fig. 3. There was no evidence of B_2O_3-assciated phases, suggesting that B_2O_3 should be dissolved in the glass matrix. An earlier study has demonstrated that B_2O_3 acts as sintering aid but it neither reacts nor dissolves in anorthite crystals.[20]

Fig. 8 shows typical microstructures of the investigated compositions after heat treatment at 920 °C (2 μm) and 950 °C (10 μm). Characteristic twined and lamellar crystals of anorthite were cemented with residual glass. The preparation of the samples for SEM observation by chemical etching with HF-solution allowed us to draw out qualitative conclusions about the chemical durability of the residual glass phase, and it was found that it follows the general order A < B < C (i.e. longer etching time was needed to sufficiently dissolve the glassy phase in samples C than in samples A). Prismatic crystals of ∼1 μm in length and an aspect ratio of 4–6 were observed in the samples made of glass powder with 2 μm in size (Fig. 8a, c and e). Less amount of glassy phase and formation of lamellar plates along with prismatic crystals (∼3 μm in the length) were observed in the samples produced from the glass powders with particle size of 10 μm (Fig. 8b, d and f). The small diameter of the EDS-spot enable performing chemical analysis only of the big lamellar plates and the prismatic crystals (Fig. 8d and f). According to these analyses, the estimated oxides contents (in wt.%, CaO 18.82–23.82, Al_2O_3 33.05–35.89 and SiO_2 43.09–45.34) correspond approximately to stoichiometric anorthite (CaO 20.16, Al_2O_3 36.65, SiO_2 43.19).

From dilatometry, the coefficient of thermal expansion (CTE) of the sintered specimens was measured

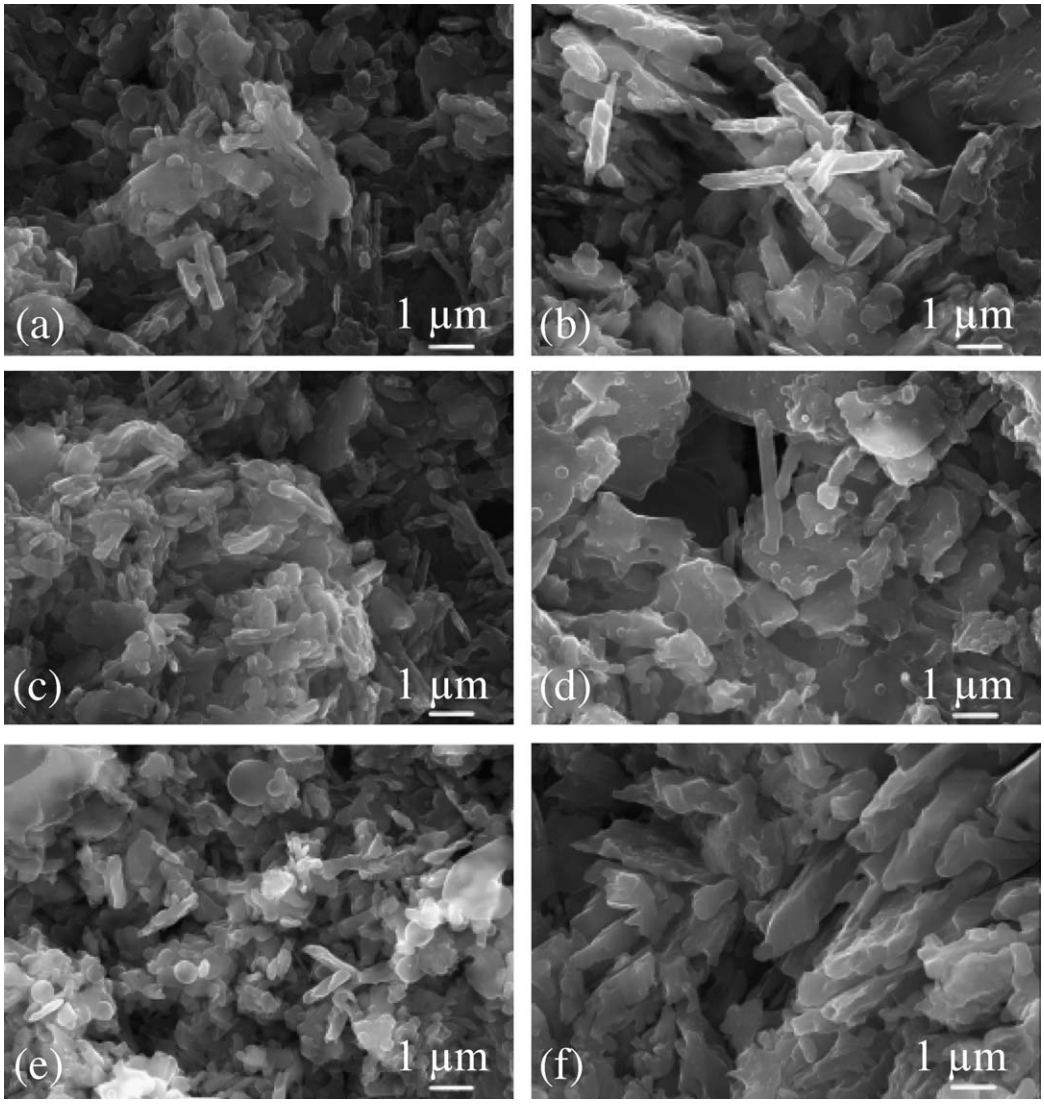

Fig. 8. Microstructure of glass-ceramics: (a) A-2 μm-920 °C, (b) A-10 μm-950 °C, (c) B-2 μm-920 °C, (d) B-10 μm-950 °C, (e) C-2 μm-920 °C, (f) C-10 μm-950 °C (dwell 1 h; etching with 2 vol.% HF).

Table 3
Properties of the synthesised anorthite based glass-ceramics A, B and C

Properties	A (An90-D10)		B (An80-D20)		C (An70-D30)	
	2 μm	10 μm	2 μm	10 μm	2 μm	10 μm
Sintering temperature (°C)	850	900	850	900	850	900
Density (g/cm^3)	2.59	2.58	2.64	2.64	2.68	2.70
Shrinkage (%)	13.70	13.40	14.35	14.45	14.70	13.10
Water absorption (%)	0.17	0	0	0.08	0	0
Bending strength (MPa)	115	111	130	116	140	125
CTE (10^{-6} K^{-1})						
100–400 °C		4.18		4.69		4.75
100–500 °C		4.62		5.05		5.10

as 4.62–5.10 × 10^{-6} K^{-1} (100–500 °C), which generally increased from composition A to B and C. These values are very close to the CTE of stoichiometric anorthite (4.5 × 10^{-6} K^{-1}) and close to the CTE of Si (3.0 × 10^{-6} K^{-1}). The properties of the produced A, B and C glass-ceramics are presented in Table 3.

In conclusion, dense anorthite based glass-ceramics with desirable physical, mechanical and thermal (CTE) properties for LTCC applications can be successfully synthesized at 850–900 °C. Investigation of electrical properties is currently underway. With regards to economical issues, in this study melting of glasses was carried out at considerably lower temperatures (1500–1580 °C) and shorter dwelling times (1.5 h) than in other similar cases reported in literature (i.e. 1600–1650 °C for 2–10 h).[6,8,10,20]

4. Conclusions

Anorthite based glass-ceramics of glass compositions located close to the anorthite-rich corner at the fluorapatite–anorthite–diopside ternary system (A, B and C) were successfully fabricated. Doping with B_2O_3 aimed at enhancing both melts' fluidity and sinterability of glass-powder compacts.

Melting at 1500–1580 °C for 1.5 h and subsequent quenching resulted in transparent, bubble free and colourless glass frits. The dependence of the thermal analysis results (DTA) on the particle size of the powders indicates that crystallization occurs via surface crystallization mechanism. Anorthite predominantly crystallized in the range of 850–950 °C along with traces of fluorapatite. Diopside was registered in compositions B and C, more pronouncedly in C.

The specimens made of fine sized powder (2 μm) were fully densified at 825 °C and exhibited the highest bending strength at 850 °C, but density significantly decreased upon heat treating at higher temperatures. The samples made of coarser powder (10 μm) exhibited quite stable values of density, shrinkage and bending strength within a wide temperature range from 825 to 900 °C. Bending strength increases in the order A < B < C. The highest values were 112–115 MPa for A, 122–130 MPa for B and 131–140 MPa for C. The CTE of the sintered specimens was 4.62–5.10 × 10^{-6} K^{-1} (100–500 °C) and generally increased from composition A to B and C.

Acknowledgements

This study was supported by CICECO and the Portuguese Foundation for Science and Technology (FCT).

References

1. Cava, J., Dielectric materials for application in microwave communications. *J. Mater. Chem.*, 2001, **11**, 54–62.
2. Niwa, K., Kamehara, N., Yokoyama, H. and Kurihara, K., Multilayer ceramic circuit board with copper conductor. In *Advances in Ceramics*, ed. J. B. Blum and W. R. Cannon. *Multilayer Ceramic Devices, vol. 19*. American Ceramic Society, Westerville, OH, 1986, pp. 41–48.
3. Chen, G. and Liu, X., Fabrication, characterization and sintering of glass-ceramics for low-temperature co-fired ceramic substrates. *J. Mater. Electr.*, 2004, **15**, 595–600.
4. Gdula, R. A., Anorthite ceramic dielectrics. *Am. Ceram. Soc. Bull.*, 1991, **50**, 555–557.
5. Kobayashi, Y. and Kato, E., Low-temperature fabrication of anorthite ceramics. *J. Am. Ceram. Soc.*, 1994, **77**, 833–834.
6. Lo, C. L. and Duh, J. G., Low-temperature sintering and microwave dielectric properties of anorthite-based glass ceramic. *J. Am. Ceram. Soc.*, 2002, **85**, 2230–2235.
7. Ryu, B. and Yasui, I., Sintering and crystallization behaviour of a glass powder and block with composition of anorthite and microstructure dependence of its thermal expansion. *J. Mater. Sci.*, 1994, **29**, 3323–3328.
8. Park, H. C., Lee, S. H., Ryu, B. K., Son, M. M., Lee, H. S. and Yasui, I., Nucleation and crystallization kinetics of $CaO–Al_2O_3–2SiO_2$ in powdered anorthite glass. *J. Mater. Sci.*, 1996, **31**, 4249–4253.
9. Padture, N. P. and Chan, H. M., On the constrained crystallization of synthetic anorthite ($CaO–Al_2O_3–2SiO_2$). *J. Mater. Res.*, 1992, **7**, 170–177.
10. Lo, C. L., Duh, J. G. and Chiou, B. S., Low temperature sintering and crystallization behaviour of low loss anorthite-based glass-ceramics. *J. Mater. Sci.*, 2003, **38**, 693–698.
11. Leonelli, C., Manfredini, T., Paganelli, M., Pozzi, P. and Pellacani, G. C., Crystallization of some anorthite-diopside glass precursors. *J. Mater. Sci.*, 1991, **26**, 5041–5046.
12. Tulyaganov, D. U., Phase equilibrium in the fluroapatite–anorthite–diopside system. *J. Am. Ceram. Soc.*, 2000, **83**, 3141–3146.

13. Tulyaganov D. U. *Theoretical and technological principles of glass-ceramic technology in the Ca5(PO4)3F-CaAl2Si2O8-CaMgSi2O6 System*. Doctoral thesis. Chemical Technological Institute, Tashkent, 1994 (in Russian).
14. Ray, C. S., Yang, Q., Huang, W. and Day, D. E., Surface and internal crystallization in glasses as determined by differential thermal analysis. *J. Am. Ceram. Soc.*, 1996, **79**, 3155–3160.
15. Höland, W. and Beall, G., *Glass-Ceramic Technology*. The American Ceramic Society, Westerville, Ohio, 2002.
16. Barbieri, L., Bonamartini Corradi, A., Lancellotti, I., Leonelli, C. and Montorsi, M., Experimental and computer simulation study of glasses belonging to diopside–anorthite system. *J. Non-Cryst. Sol.*, 2004, **345–346**, 724–729.
17. Tulyaganov, D. U., Agathopoulos, S., Ventura, J. M., Karakassides, M. A., Fabrichnaya, O. and Ferreira, J. M. F. Synthesis of glass-ceramics in the CaO–MgO–SiO_2 system with B_2O_3, P_2O_5, Na_2O and CaF_2 additives. *J. Eur. Ceram. Soc*., in press.
18. Torres, F. J. and Alarcon, J., Mechanism of crystallization of pyroxene-based glass-ceramic glazes. *J. Non-Cryst. Sol.*, 2004, **34**, 45–51.
19. Tulyaganov, D. U., Agathopoulos, S., Fernandes, H. R. and Ferreira, J. M. F. Processing of glass-ceramics in the SiO_2–Al_2O_3–B_2O_3–MgO–CaO–Na_2O–(P_2O_5)–F system via sintering and crystallization of glass powder compacts. *Ceram. Int*., in press.
20. Lo, C. L., Duh, J. G., Chiou, B. S. and Lee, W. H., Microstructure characteristics for anorthite composite glass with nucleating agents of TiO_2 under non-isothermal crystallization. *Mater. Res. Bull.*, 2002, **37**, 1949–1960.